This article has been accepted for publication in a future issue of this journal, but has not been fully edited. Content may change prior to final publication. Citation information: DOI 10.1109/JSEN.2018.2795046, IEEE Sensors Journal

An Electromagnetic Sensor Prototype to Assist Visually Impaired and Blind People in Autonomous Walking

E. Cardillo, V. Di Mattia, G. Manfredi, P. Russo, A. De Leo, A. Caddemi, G. Cerri

***Abstract*—The feasibility of an electromagnetic sensor to assist the autonomous walking of visually impaired and blind users is demonstrated in this paper. It is known that people affected by visual diseases usually walk assisted by some supports, among which the white cane is the most common. Our idea consists in applying a microwave radar on the traditional white cane making aware the user about the presence of an obstacle in a wider and safer range. Compared to the already existing Electronic Travel Aids devices, the proposed system exhibits better performance, noise tolerance and reduced dimensions. In the following, the latest developments of this research activity are presented, with special concern for the miniaturization of circuit board and antennas. A laboratory prototype has been designed and realized and the first test results of obstacle detection are hereby shown to demonstrate the effectiveness of the system.**

***Index Terms*— electronic travel aids, visually impaired assistance, autonomous walking, short-range radar, pulse compression technique.**

I. Introduction

As it is well known, people affected by blindness and visual diseases need to use special devices to overcome daily tasks, e.g. moving and navigating around unfamiliar environments. Usually, blind people walk assisted by supports ranging from the traditional white cane to more technological devices, namely Electronic Travel Aids (ETA) [1, 2]. Such systems are mainly based on ultrasonic or optic sensors, whereas the use of the electromagnetic (EM) technologies to develop a support system for visually impaired people is a research topic currently under development [3].

It is generally agreed that neither ultrasonic nor optical ETA's satisfy all the needs of a visually impaired person. The ultrasonic ETA's exhibit a limited operating range due to problems when operating with highly reflective surfaces e.g. smooth surfaces, with a low incidence angle of the beam and when detecting small openings, e.g. a narrow door.

E. Cardillo and A. Caddemi are with the Dept. of Engineering, Università di Messina, 98166, Messina, Italy; email: ecardillo@unime.it; acaddemi@unime.it

V. Di Mattia, G. Manfredi, P. Russo, A. De Leo, G. Cerri are with the Dept. of Information Engineering, Università Politecnica delle Marche, Ancona, Italy; email: v.dimattia@univpm.it; g.manfredi@univpm.it; paola.russo@univpm.it; a.deleo@univpm.it; g.cerri@univpm.it

The optical ETA's do not suffer from similar drawbacks, but are affected by a high sensitivity to the natural ambient light or by the dependence on the optical characteristics of the target.
The most recent ETA devices employing an electromagnetic (EM) sensor have been proposed in [4, 5], both showing a 24 GHz frequency modulated continuous wave (FMCW) radar able to detect short-range targets.

In [4], the radar is shown to be successfully usable for different industrial and medical applications. One of these applications regards the possibility of augmenting the reality of visually impaired people by navigating through their daily lives. It is proposed that a radar sensor scans the environment, then the target angle and distance information are collected, evaluated and mapped into the audio space by using virtual 3D audio rendering techniques. A FMCW radar has been used in [5] with the aim of realizing a device to be mounted on a white cane. Great attention has been paid to the antenna design, but no details on the system performances nor evidence of proofs with actual end users have been reported.

In this context, our preliminary studies had previously concerned the comparison between the performances of an EM system and those of the traditional supports [6]. This type of investigation had never been presented in the literature, thus representing a pioneer research activity on the expected advantages coming from the adoption of the EM technology as an aid for visually impaired users. Briefly, such preliminary investigations demonstrated the potential for the EM technology in terms of resolution, efficiency and comfort for the user. Since the very first tests were carried out by using laboratory instrumentation, recently our attention has been focused on the realization of a cost-effective compact radar system characterized by a suitable performance.

The main idea is to realize a device small enough to be attached onto the white cane to enhance the usefulness of a traditional and widely accepted travel aid [7, 8]. As a matter of fact, when realizing a novel support for disable people, it is important not to forget the personal considerations and impressions of end users. The positive reception of a new device within the blind community is a very critical issue. Most requirements concern aesthetics characteristics and appearance: they should be unobtrusive, unnoticeable and easy to carry [9]. For such reasons we chose to design a small and user-friendly

This article has been accepted for publication in a future issue of this journal, but has not been fully edited. Content may change prior to final publication. Citation information: DOI 10.1109/JSEN.2018.2795046, IEEE Sensors Journal

component integrated onto the white cane, the most widely used and accepted system, in order to make the user more confident and eager to try the new technology.

Starting from the laboratory set up used for the first tests, the attention has been paid on the reduction of the antenna dimensions, which implies the use of a higher frequency, as well as on the miniaturization of the circuit board. Some aspects and preliminary results of such optimization process have already been described in [8]. In this paper, the last improvements, together with the realization and testing of the first complete laboratory prototype are reported.

In detail, Section II defines the design requirements, Section III gives an overview of proposed system and its application, Sections IV and V explain the antenna design, realization and its experimental validation, respectively. Then, Section VI reports some laboratory measurements carried out by using the final prototype for testing the system performances and efficiency. To conclude, in Section VII some discussion and hints for future improvements are proposed.

II. System Requirements

The system works as a short-range radar and has to satisfy the following requirements, arising from the specific and innovative type of application:

1. small dimensions and reduced weight, to preserve the user's comfort and to promote the acceptability of a new device;
2. working frequency inside the free-use band for short-range radar applications as defined by the national and international regulations [10]. A resolution of about 10-20 cm is required, which implies a frequency bandwidth of about 1 GHz;
3. radiation pattern shaped as a vertical fan beam, narrow over the horizontal plane ($\leq 10°$) and wide over the vertical one (about 40°), as schematically depicted in Fig. 1. Over the azimuthal plane, the direction of the obstacle is detected by scanning the environment with the classical horizontal motion of the cane. This scenario has been described in Fig. 1a. Over the elevation plane, as shown in Fig. 1b, the wide beam allows even the detection of suspended obstacles, e.g. the branch of a tree;
4. observation range from 1 m to 5 m. Such limits have been arbitrarily chosen according to the end user needs. Indeed, the radar is designed to be mounted on the white cane, which efficiently works for very short distances (< 1 m). The upper limit of 5 m is a tradeoff between the need to efficiently warn the user about the presence of obstacles, and the risk of annoying him with warnings due to very far targets. Our system is able of generating a maximum output power of 11 dBm. This value complies with the international regulations regarding the exposure to EM fields [11]. Accordingly, at a distance of 1 m from the antenna (a reasonable minimum distance considering the presence of the white cane) the regulation imposes a maximum E field of 6 V/m, which in our case corresponds to a maximum power of 15 dBm.

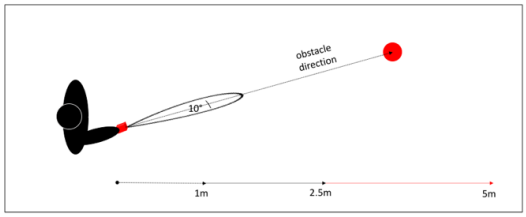

(a)

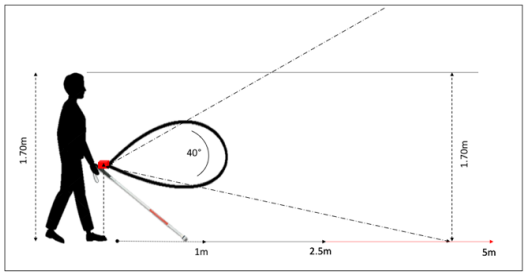

(b)

Fig 1. Schematic representation of the EM beam shape due the radar mounted onto a white cane showing (a) top and (b) lateral view.

III. Radar Overview

The proposed radar application concerns a short-range environment for which a pulsed frequency-modulated waveform has been preferred. By adopting a classic echo radar mode, the shorter the pulse width, the better the resolution [12]. Thus, for detecting targets within a few meters with, a pulse duration lasting nanoseconds is needed, requiring an expensive and complex pulse generator. On the other hand, a pulsed signal allows switching off the transmitter during the echo listening time, thus drastically reducing the power consumption. For fulfilling both requirements, i.e. high resolution and low power consumption, a pulsed chirp scheme has been adopted, thereby managing the spatial resolution in terms of the frequency modulation bandwidth [13]. The chirped waveform has been obtained by using a modulating saw-tooth signal with a period of 2 ms and a suitable amplitude for generating a 1.1 GHz frequency bandwidth Δf, from 24.0 to 25.1 GHz. Such a bandwidth will result in a spatial resolution of 14 cm, which satisfies the design requirement. With the aim of achieving both a reasonable dwell time and a limited ON state period of the transmitter, the pulse duration has been chosen equal to 10 ms. Similarly, the pulse repetition time (PRT) has been selected equal to 100 ms, thus obtaining a duty-cycle of 10% which is a good compromise between the requirements of energy saving and a comfortable data refresh time for human people. These performances have been obtained by realizing a cost-effective system based on commercially available components and a microwave section employing microstrip technology that allows ease of integration with the antenna section as well as the prototype realization by using in-house facilities. With the aim of providing a feedback signal to the user, a vibrational and/or acoustic warning, is generated every time an obstacle is detected.

The proposed radar architecture adopts the BGT24MTR11

integrated circuit as leading block, a SiGe MMIC Transceiver by Infineon Technologies AG [14]. By means of its 24.0 GHz Voltage Controlled Oscillator (VCO), it can operate from 24.0 to 26.0 GHz delivering a main RF output power of 11 dBm, which is the maximum provided by this chip. A demo board for the XMC4500 microcontroller (MCU) by Infineon Technologies AG has been used both to drive the system and to perform data processing (Fig. 2).

The working principle is straightforward. A balanced TX antenna and an unbalanced RX antenna have to be connected to the transceiver board equipped with microstrip matching networks, as described in the component datasheet. The echoed signal reaches the homodyne receiver, whose IF output is first digitized and then processed with a Fast-Fourier Transform (FFT) with Hamming window. Lastly, a maximum search algorithm is applied with the aim of locating the nearest signal peak and consequently the target distance.

This procedure allows obstacle detection and then, after a comparison with a predefined threshold, user alert about the presence of hazards.

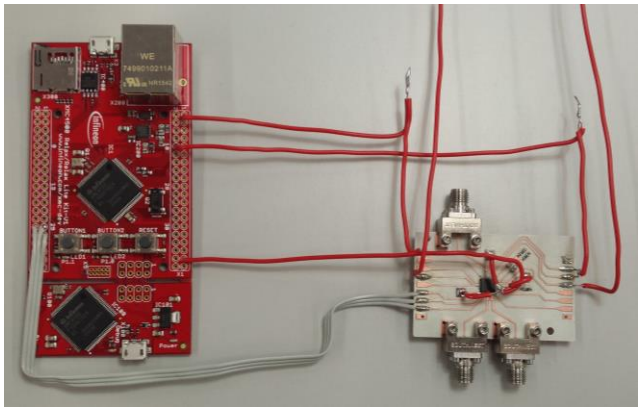

Fig. 2. Photo of the demo board used both to drive the system and to perform data processing.

In Table I, a comparison among the performances of such radar devices as proposed in the literature [3, 4], is summarized. The main strengths of the present system are: a) better resolution; b) lower power consumption.

TABLE I
COMPARISON BETWEEN NEWEST RADARS FOR BLIND PEOPLE

Parameters	Smart EM cane	VTT radar	FMCW Radar
Chipset	BGT24MTR11	BGT24MTR12	BGT24MTR11
Frequency Bandwidth (GHz)	24 – 25.1	24 – 24.25	24 – 24.25
Radar range (m)	5	37.5	/
Resolution (cm)	14	60	60
TX Antennas	planar patch array, balanced, vertical fan shaped radiation pattern	planar patch array, unbalanced	planar patch array, balanced, vertical fan shaped radiation pattern
RX Antenna	planar patch array, unbalanced, vertical fan shaped radiation pattern	two planar patch array, balanced	planar patch array, unbalanced, vertical fan shaped radiation pattern.
Radiated power (dBm)	11	8	11
Transmitted signal	Pulsed frequency modulated wave: reduced consumption; reduced EM compatibility issues	Continuous wave: significant power consumption; possible EM compatibility issues	Continuous wave: significant power consumption; possible EM compatibility issues
Warning type	Acoustic + vibrational	Vibrational	/
Stigma	To be attached onto white cane, nothing to separately control, no device to wear	Chest belt to wear	To be attached onto white cane, nothing to separately control, no device to wear

IV. ANTENNA DESIGN

The BGT24MTR11 integrated circuit presents a radar architecture characterized by a differential output and a single-ended input. Therefore, a balanced TX antenna and an unbalanced RX antenna have been designed. Furthermore, bearing in mind the technical requirements listed in Section II, we chose to use series fed microstrip patch arrays because of their important advantages: lightweight, low volume and thin profile configurations, low fabrication cost, easy integration with the microwave circuit and matching networks.

A. Simulation overview

The design of both the TX and the RX antennas has been carried out by using the CST Microwave Studio® software [15]. First, the dielectric substrate has been selected to obtain a robust structure together with a wide bandwidth and a good radiation efficiency. The Arlon 25N laminate, characterized by a thickness of 1.52 mm and a dielectric constant of 3.38, has been preferred. Then, the geometrical parameters of a single patch have been approximately defined, according to the operating frequency f = 24.5 GHz. The patch length L has been

This article has been accepted for publication in a future issue of this journal, but has not been fully edited. Content may change prior to final publication. Citation information: DOI 10.1109/JSEN.2018.2795046, IEEE Sensors Journal

chosen equal to half-wavelength λ_g (3.33 mm), whereas the patch width W has been calculated equal to 4.17 mm [16]. In order to improve the typical low gain of a single patch, an array of N elements has been realized. The suitable number of radiating elements has been defined by assuming the whole array as an equivalent aperture antenna. From antenna theory, it is known that in order to obtain the desired half power beam width (HPBW) over horizontal plane, i.e. 10°, it is necessary to satisfy the following relationship.

$$HPBW = 10° = \frac{51°}{a} \quad (1)$$

where a is the larger dimension of the rectangular aperture. Equation (1) gives $a \cong 5\,\lambda \cong 6\,cm$. Furthermore, since each patch is 3.33 mm long and has to be $\lambda_g/2$ apart from the adjacent one, N = 9 is obtained for a broadside radiation at the desired frequency.

B. *Transmitting Antenna*

Due to the differential output of the transmitter, a balanced TX antenna has been designed. To this end, the configuration shown in Fig. 3 has been chosen. It consists of two parallel linear fed series arrays of N = 9 elements, designed over the same dielectric substrate of the receiving antenna, but translated by $\lambda_g/2$ with respect to each other. Such a translation causes a phase shift of 180° between the fields of two arrays, hence compensating the phase shift of the feeding signals. As a consequence, all patches radiate in phase obtaining just one main lobe, as desired.

Once we established a suitable design configuration, starting from the values of a single patch, a step by step optimization process of the main parameters of the patches, such as W, L, W_w and the geometrical dimensions of the substrate (as reported in Fig. 3), has been carried out. In details, the following goals have been defined:

- S_{11} < -10 dB over a wide band, from 24 to 25 GHz;
- HPBW < 15° over the horizontal plane;
- side lobe level, S_{LL} < -10dB, both over the horizontal and the vertical plane;

The optimized values obtained at the end of this process are reported in Table II. It is worth noting that a tapering of the patch widths has been implemented to better shape the vertical fan beam and to reduce the S_{LL}.

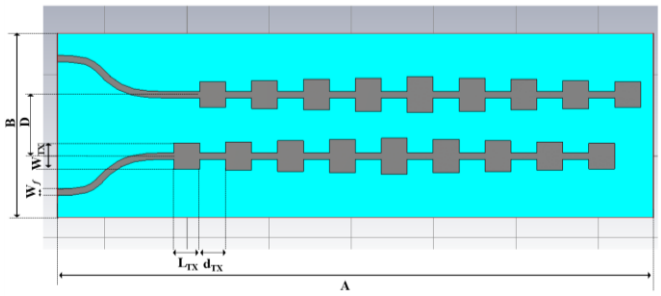

Fig. 3. Layout of the transmitting antenna.

More specifically,

$$W_{TXi} = W_{TX(N+1-i)} = a_i W_{TX1}, \text{ for i= 1,2,…,5}$$

where the a_i coefficients and the W_{TX1} values are reported in Table II with the most important radiation parameters.

In Fig. 4 the reflection coefficient demonstrating a good matching over the entire operating frequency band is reported. Moreover, Fig. 5 shows the radiation patterns over both the horizontal (left) and the vertical (right) plane, at the central frequency of 24.5 GHz. As desired, the antenna has a narrow radiation pattern over the azimuthal plane (HPBW of about 11°) and a wider beam over the elevation plane (HPBW of about 35°) thus satisfying the design requirements.

TABLE II
OPTIMIZED GEOMETRICAL PARAMETERS OF TX ANTENNA

Parameter	Values (mm)
A_{TX}	72.45
B_{TX}	22.78
D	7.56
d_{TX}	3.15
W_{TX}	3.15
L_{TX}	3.15
W_{f_TX}	1
a_1	1
a_2	1.1
a_3	1.2
a_4	1.3
a_5	1.4

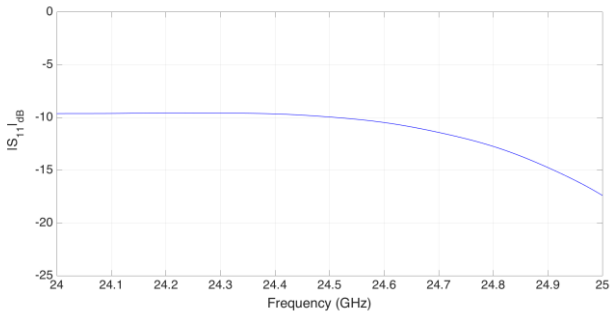

Fig. 4. Simulation of the TX antenna reflection coefficient.

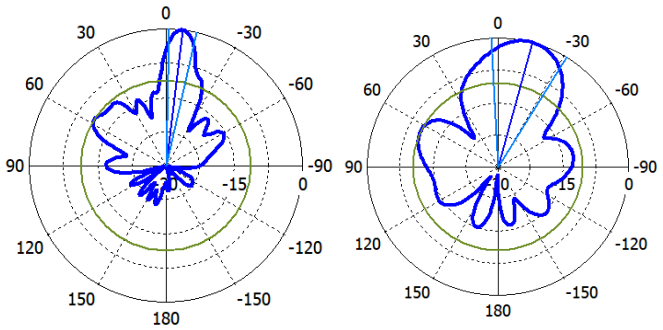

Fig. 5. Radiation patterns (at the central frequency of 24.5 GHz) of the TX antenna over the horizontal (left side) and the vertical plane (right side). All values are in dB.

The main radiation parameters are listed in Table III. The final gain of the TX antenna is lower than the desired one because the width tapering that allows a reduction of S_{LL}, also broadens the main beam thus causing a reduction of the directive gain. Nevertheless, it still reaches a satisfactory value.

TABLE III
RADIATION PARAMETERS OF TX ANTENNA AT 24.5 GHZ

Parameter	Values (mm)
Azimuthal (E-plane)	
Main Lobe Direction (deg.)	-7
Half Power Beamwidth (deg.)	11.6
Side Lobe Level (dB)	-11.3
Gain (dB)	15.2
Elevation (H-plane)	
Main Lobe Direction (deg.)	-15
Half Power Beamwidth (deg.)	35
Side Lobe Level (dB)	-10.4
Gain (dB)	13

C. *Receiving Antenna*

The chip output port is single-ended, therefore a single linear fed series array of 9 elements is employed, as shown in Fig. 6. An optimization process, as for the TX antenna, has been followed also for the RX antenna.

The optimized values for the geometrical parameters of the RX antenna are reported in Table IV.

In Fig. 7 the reflection coefficient calculated at the antenna port is reported. The diagram highlights a good matching inside the desired frequency bandwidth, according to the design requirements.

Furthermore, Fig 8. shows the radiation patterns over both the azimuthal and the elevation plane at the central frequency of 24.5 GHz., whereas the main radiation parameters are listed in Table V.

It can be easily seen that the RX antenna radiates a vertical fan beam as well as the TX antenna does

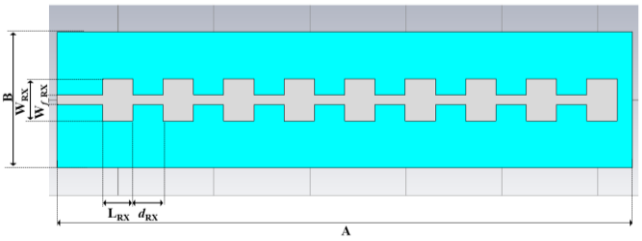

Fig. 6. Layout of the receiving antenna.

TABLE IV
OPTIMIZED GEOMETRICAL PARAMETERS OF RX ANTENNA

Parameter	Values (mm)
A_{RX}	59.85
B_{RX}	14.17
d_{RX}	3.15
W_{RX}	3.15
L_{RX}	3.15
W_{f_RX}	1

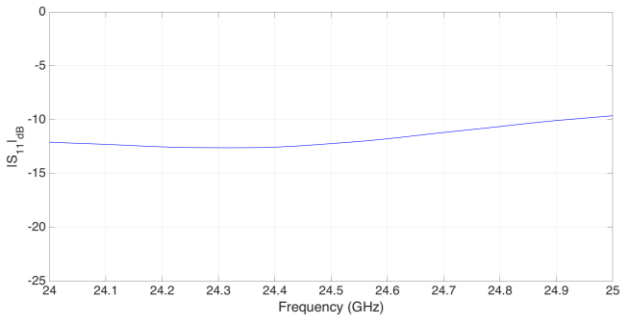

Fig. 7. Simulation of the RX antenna reflection coefficient.

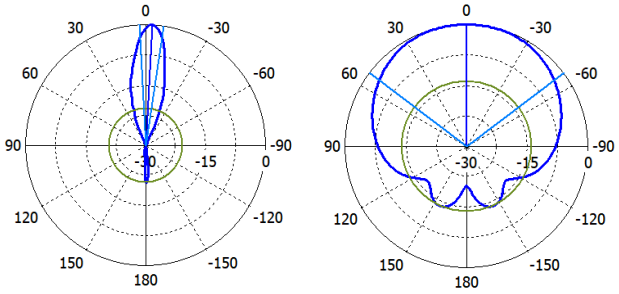

Fig. 8. Radiation patterns (at the central frequency of 24.5 GHz) of RX antenna over azimuthal plane (left side) and elevation plane (right side). All values are in dB.

TABLE V
RADIATION PARAMETERS OF RX ANTENNA

Parameter	Values (mm)
Azimuthal (E-plane)	
Main Lobe Direction (deg.)	-4
Half Power Beamwidth (deg.)	12.9
Side Lobe Level (dB)	-14.5
Gain (dB)	12.8
Elevation (H-plane)	
Main Lobe Direction (deg.)	0
Half Power Beamwidth (deg.)	105
Side Lobe Level (dB)	-13.9
Gain (dB)	11.8

Anyway, since the sensing volume of the radar system is due to the combination of both patterns of the antennas, the RX has been designed for satisfying the third system requirement, as exposed in Section II. Indeed, its small HPBW over the azimuthal plane makes the total beam sectional area narrower with respect to that of TX antenna alone. On the other hand, its large HPBW over the elevation plane leaves the total beam sectional area almost equal.

V. EXPERIMENTAL VALIDATION

After the design and optimization steps, the TX and RX antennas have been realized and tested for evaluating their actual performance.

Fig. 9 shows a comparison between the EM simulations and the measurement data.

It can be highlighted that a good agreement between such results is obtained, thus demonstrating the accuracy and reliability of the numerical simulations.

This article has been accepted for publication in a future issue of this journal, but has not been fully edited. Content may change prior to final publication. Citation information: DOI 10.1109/JSEN.2018.2795046, IEEE Sensors Journal

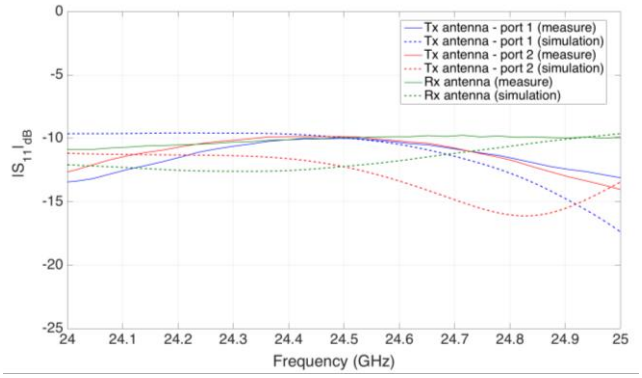

Fig. 9. S_{11} at port 1 of the TX antenna (blue); S_{11} at port 2 of the TX antenna (red); S_{11} of the Rx antenna (green).

As far as the experimental evaluation of the radiation patterns is concerned, each antenna has been placed inside an anechoic chamber and connected to a standard set up measurement, fed by a semi-rigid coaxial RF cable, as shown in Fig. 10. As a consequence, the effects of the cable on the radiation patterns have been taken into account and the actual measurement configurations have been simulated. The new simulations included the antenna fed by a waveguided port and by a semi-rigid coaxial wire (6 cm long).

In Fig. 11, the comparison between the simulation results and the measurements carried out with the RX antenna in the anechoic chamber are shown. In detail, Fig. 11 compares the three different radiation patterns obtained by:

- EM simulation of the stand-alone antenna.
- EM simulation of the antenna connected to a semi-rigid coaxial wire, 6 cm long.
- Measurement data in the anechoic chamber (antenna + cable).

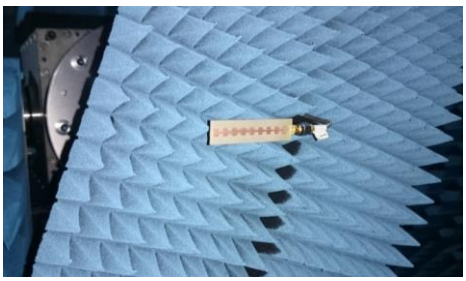

Fig. 10 Picture of the set up measurement of the RX antenna in the anechoic chamber.

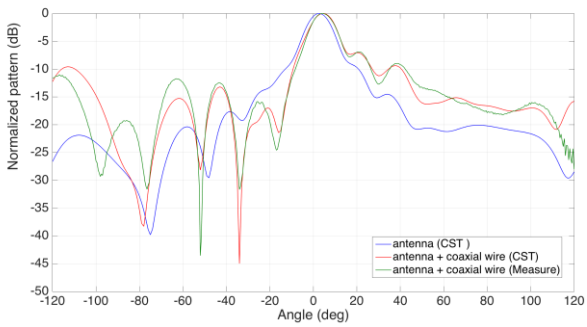

Fig. 11 Normalized radiation pattern (at the central frequency of 24.5 GHz) of the RX antenna for the horizontal plane. Measurements performed in anechoic chamber (green) and simulations: antenna without (blue) and with (red) the semi-rigid cable.

As expected, Fig. 11 shows that the measured diagram is altered, no longer satisfying all the design requirements (especially in terms of the side lobe level). By comparing this test result with the simulated diagrams, it is clear that the degradation has been caused by the coaxial semi-rigid wire, mainly affecting side angles, whereas the HPBW is unchanged.

Given the practical impossibility of a balanced feeding of the TX antenna, just one port has been excited, whereas the other one has been loaded with 50 Ω. The measured data have then been compared with EM simulation in the following conditions:

- the TX antenna fed by a balanced port
- the TX antenna fed by a semi-rigid cable and a single port.

In Fig. 12, the results in terms of the horizontal radiation patterns at the central frequency of 24.5 GHz are reported. Again, the comparison demonstrates that the variation of the measured radiation patterns is caused by the measurements set up, which has been reliably implemented within the numerical simulation.

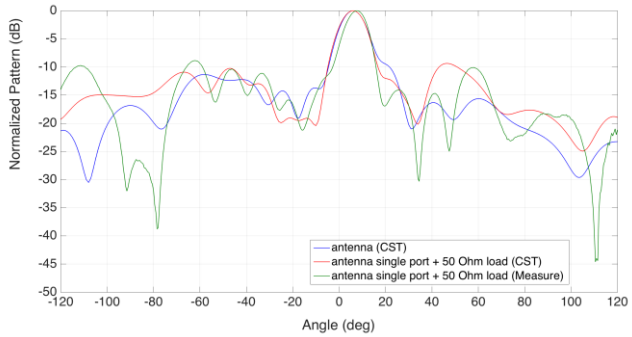

Fig. 12 Normalized radiation pattern (at the central frequency of 24.5 GHz) of the TX antenna for the horizontal plane. Measurements in anechoic chamber (green) and simulations: antenna fed by a balanced port (blue) and with (red) a semi-rigid cable and a single port.

In conclusion, all the comparisons between measurement data and simulation results concerning the same set up configuration show a very good agreement, thus demonstrating that the designed and simulated antenna models are accurate and reliable.

VI. Radar Board and Measurements

In Fig. 13, a picture of the final laboratory prototype, including the radar architecture, the two antennas and all the RF connections, is shown.

In order to define the minimum detectable signal, a preliminary measurement without targets has been performed. The poor isolation between transmitter and receiver leads to the crosstalk noise level, clearly visible in Fig. 14. In order to account for this noise level, and hence for the minimum detectable signal, a threshold has been set at twice the level of the crosstalk noise (in order to guarantee a guard level), as highlighted in Fig. 14. Each signal measured by the radar system is normalized to the maximum value of such noise and each echo larger than the noise threshold is associated to an obstacle

This article has been accepted for publication in a future issue of this journal, but has not been fully edited. Content may change prior to final publication. Citation information: DOI 10.1109/JSEN.2018.2795046, IEEE Sensors Journal

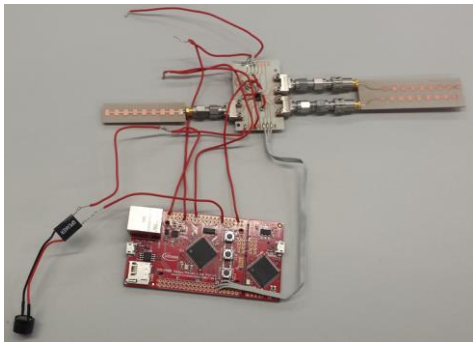

Fig. 13. Photo of the radar laboratory prototype.

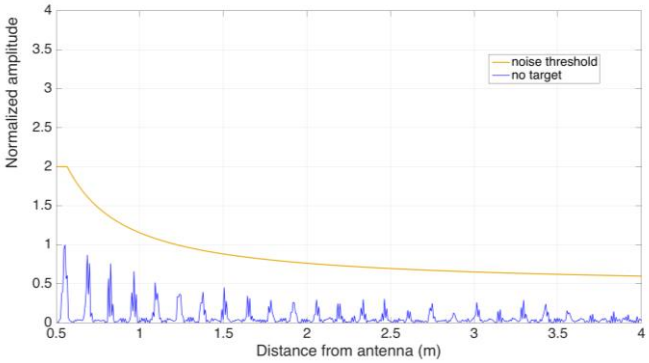

Fig 14 Crosstalk noise (blue) and threshold level (yellow).

Then, several measurements have been carried out in order to verify the system performance in a real environment, by locating the radar at the height of 1 m from the ground since this is expected to be the final position on the white cane handle.

A cylindric metallic target (1.75 m height and 7.5 cm diameter) has been placed at increasing distances from the radar, ranging from 0.5 m to 3.5 m, as shown in Fig. 15. Despite the design requirement, the upper limit is currently limited to 3.5 m because of two main reasons: losses in the microwave connections (around 2 dB) and missing amplification stage at the intermediate frequency in the receiver chain (it will be added to the final prototype).

Another set of measurements has been performed for confirming the radar capability of detecting targets with a very high horizontal selectivity.

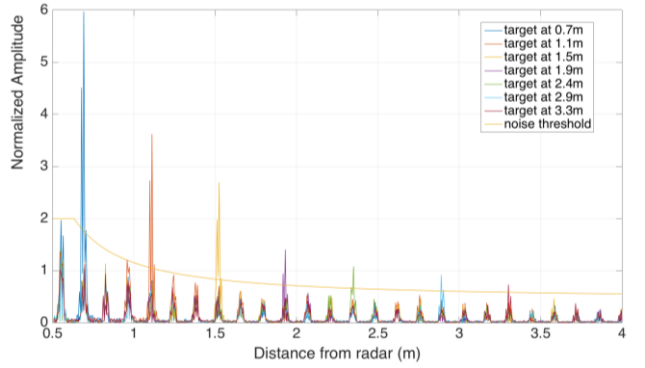

Fig. 15. Radar signals obtained by moving a cylindric metallic obstacle from a distance of 50 cm up to 3.5 m with respect to the antenna. The noise threshold (yellow line) is shown.

The FFT data related to the IF frequency signal have been extracted from the MCU memory. In Fig. 16 such data are reported for different angular positions of the target over the horizontal plane, together with the corresponding value of the threshold noise. The same cylindric reflecting obstacle used in the previous tests and located at a distance of 1.5 m from the radar has been used. It is seen that the target can be correctly detected within an angular sector of +/- 3° with respect to the main lobe position, whereas it is almost undetectable at +/- 7° where the signal level is masked by the cross-talk noise. These results confirm the high spatial selectivity of the system.

Afterwards, the capability of detecting obstacles suspended at different heights with respect to the radar has been tested. The radar has been located one meter above the ground whereas the cylindric obstacle has been moved along different vertical angular positions, according with the design requirements defined in Section II.

Indeed, since using the bare white cane typically allows detection of obstacles lying on (or close to) the ground, it is extremely important to design a device able to protect the user against collisions with obstacles located at different elevations. Once again, a very good performance of the system has been observed since the radar has proven its ability to detect the presence of a suspended obstacle, according to the aperture of the TX radiation pattern. Indeed, the vertical location of the target can be correctly detected within an angular sector of +/- 17°. The related measurement results are shown in Fig. 17.

As explained in Section IV, the total beam of the radar system is due to the combination of both the TX and the RX radiation patterns. The results presented in Figs. 16-17 demonstrate that both antennas have been efficiently designed and optimized, because the requirements on azimuthal and elevation apertures are fully satisfied. The system capability of detecting obstacles of different shapes, dimensions and materials has been tested, as a preliminary demonstration of the usefulness of such system for daily tasks. In particular, a wooden chair, a chest of drawers and a human subject have been considered. All of them, located at the distance of 1.5 m from the radar have shown to be easily detectable, since their echoes are sensibly greater than the noise threshold, as shown in Fig. 18.

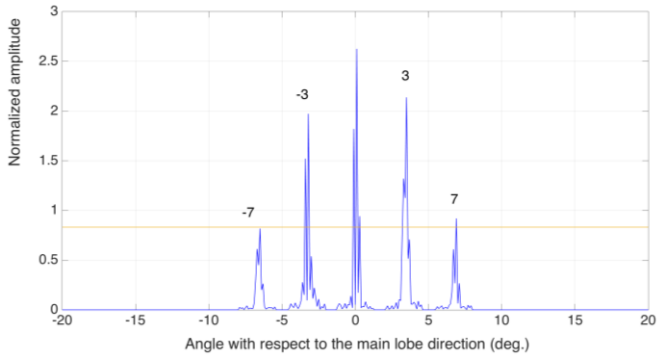

Fig. 16. Echo IF amplitude for target horizontal angular positions of 0° (a), -3° (b), 3° (c), -7° (d) and 7°(e), respectively.

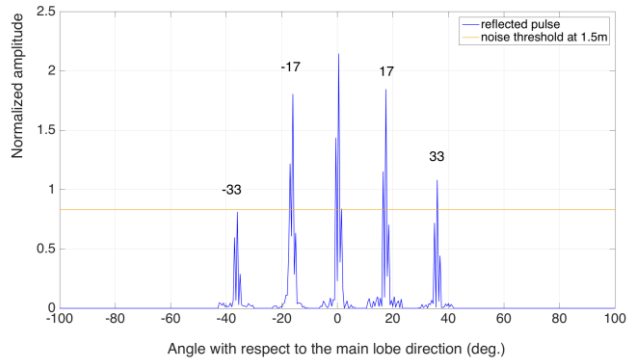

Fig. 17. Echo IF amplitude for target vertical angular positions of -4° (a), -4° (b), -7° (c) and 7° (d), respectively.

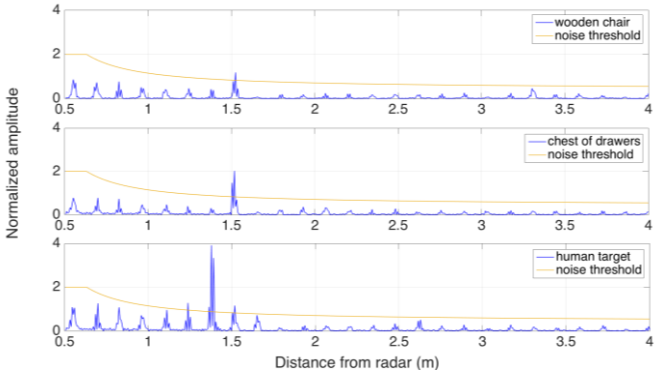

Fig. 18. Example of radar signals obtained in presence of different obstacles located at 1.5 m from the system. From the top to the bottom, a wooden chair, a chest of drawers and a human target are detected.

VII. Conclusions

This paper discusses the realization of an EM travel support for visually impaired people. Starting from the encouraging results of previous research activities, the project has been recently growing up to the realization of a short range radar system to be mounted on a traditional white cane.

Such goal has been achieved by realizing a cost-effective system based on commercially available components and a microwave section based on microstrip technology that allows ease of integration with the homemade antennas as well as the prototype realization by using in-house facilities.

To this end, it is important to underline that some aspects have to be improved. First of all, it is necessary to extend the observation range fully up to 5 m either by reducing the losses in the microwave connections and by introducing an amplification stage at the intermediate frequency in the receiver chain.

Furthermore, the suitability of the system needs to be improved by integrating all the subunits over the same circuit board.

We estimate to obtain a final prototype with the appearance of a small box of about 10 cm and weight of a few hundreds of grams, easy attachable to the handle of the white cane. Furthermore, considering that the components have been selected with the goal of realizing a portable system, the final prototype will be able to provide the user with a full day of autonomy (about 12 hours).

VIII. Acknowledgement

The Authors wish to thank Infineon Technologies Italia S.r.l. for providing technical support, and Dr. Andrea Schiavoni of Telecom Italia Lab for his valuable help in anechoic chamber measurements.

References

[1] D. Dakopoulos and N. G. Bourbakis, "Wearable Obstacle Avoidance Electronic Travel Aids for Blind: A Survey", *IEEE Trans on systems, man, and cybernetics—Part c: Applications and reviews*, 40, 1, (2010)

[2] Roentgen, Uta R.; Gelderblom, Gert Jan; Soede, Mathijs; de Witte, Luc P. "The Impact of Electronic Mobility Devices for Persons Who Are Visually Impaired: A Systematic Review of Effects and Effectiveness", I, 103, 11, 743-753, (2009).

[3] V. Di Mattia, L. Scalise, V. Petrini, P. Russo, A. De Leo, E. Pallotta, A. Mancini, P. Zingaretti And G. Cerri, "Electromagnetic technology for a new class of electronic travel aids supporting the autonomous mobility of visually impaired people", I" Nova Science Publishers, Inc. 2016.

[4] S. Jardak, T. Kiuru, M. Metso, P. Pursula, J. Häkli, M. Hirvonen, S. Ahmed, M. Alouini "Detection and localization of multiple short range targets using FMCW radar signal," *2016 Global Symposium on Millimeter Waves (GSMM) & ESA Workshop on Millimetre-Wave Technology and Applications*, Espoo, 2016, pp. 1-4.

[5] S. Pisa, E. Pittella, and E. Piuzzi, "Serial Patch Array Antenna for an FMCW Radar Housed in a White Cane," *International Journal of Antennas and Propagation*, vol. 2016, Article ID 9458609, 10 pages, 2016.

[6] L. Scalise, V. Primiani, P. Russo, D. Shahu, V. Di Mattia, A. De Leo, G. Cerri, "Experimental investigation of electromagnetic obstacle detection for visually impaired users: a comparison with ultrasonic system", *IEEE Transactions on Instrumentation and Measurement*, vol. 61, issue 11, pp. 3047-3057, Nov. 2012.

[7] V. Di Mattia, V. Petrini, M. Pieralisi, G. Manfredi, A. De Leo, P. Russo, L. Scalise, G. Cerri. "A K-band miniaturized antenna for safe mobility of visually impaired people", *IEEE 15th Mediterranean Microwave Symposium (MMS), Lecce*, 2015, pp. 1-4.

[8] V. Di Mattia, G. Manfredi, A. De Leo, P. Russo, L. Scalise, G. Cerri, A. Caddemi, E. Cardillo, "A feasibility study of a compact radar system for autonomous walking of blind people", *IEEE 2nd International Forum on Research and Technologies for Society and Industry Leveraging a better tomorrow (RTSI)*, Bologna, 2016, pp. 1-5.

[9] Hersh, Marion and Johnson, Michael A. (Eds.). 2008. *Assistive Technology for Visually Impaired and Blind People*, Springer-Verlag London, ISBN: 1846288665 9781846288661.

[10] Commission Implementing Regulation (EU) No 485/2011 of 18 May 2011, Official Journal of the European Union 133, 20.5.2011.

[11] D.M. 381/98, Sept. 10 1998.

[12] M. Skolnik, "Introduction to Radar systems," 3rd ed., McGraw-Hill Co., New York, 2002.

[13] M. A. Richards, J. A. Scheer, W. A. Holm, "Principles of Modern Radar: Basic principles," SciTech Publishing, 2010.

[14] ISM Infineon BGT24MTR11 datasheet, Rev. 3.1, 2014-03-25.

[15] www.cst.com.

[16] Constantine A. Balanis. 2005. *Antenna Theory: Analysis and Design*. Wiley-Interscience.

Emanuele Cardillo (M'15) received his MSc degree in Electronic Engineering from the University of Messina, Italy, in 2013. He is currently pursuing the PhD degree in the microwave electronics field at the University of Messina. His current research interests are focused on the microwave electronics field, mainly on the design of active and passive planar hybrid microwave integrated circuits (HMIC), linear and noise modeling of microwave field-effect transistors, linear and noise microwave measurements (1 - 50 GHz), design of micro-radar systems and realization of HMIC circuits and systems He served as member of the organizing committee of the

International Workshop on Integrated Nonlinear Microwave and Millimetre-wave circuits (INMMIC 2015). He serves as permanent member of the scientific committee of the International Conference on Microelectronic, Devices and Technologies (MicDAT).

Valentina Di Mattia received her M.S. degree (cum laude) in Clinical and Biomedical Engineering at "Sapienza", University of Rome in 2009 and her Ph.D. in "Bioengineering and Electromagnetism" at Università Politecnica delle Marche, Ancona, in 2014. Currently, she is a research fellow at the Department of Information Engineering of the same University and her main research activities focus on the design of: electromagnetic devices for contactless monitoring of human vital signs, indoor localization and tracking; small systems to support the autonomous walking, or running, of visually impaired people and athletes. In particular, her expertise concerns the simulation, optimization and testing of small antennas working at high frequencies. She is a member of Siem, Italian society of electromagnetism

Giovanni Manfredi received the B.S. degree in electronic engineering from the University of Messina, in 2010, the M.S. degree in electronic engineering from the University of Rome "La Sapienza" in 2013, and the Ph.D in information engineering from the University Polytechnic of Marche, in 2017.
He currently works as Research Fellow at the french aerospace lab of Paris, ONERA. His recent activities have included developing of an electromagnetic model, based on physical optics, to characterize the reflected field by a human body and utilizing this system for the Doppler analysis of the signature of human motion

Paola Russo received the Ph.D. degree in electronic engineering from the Polytechnic of Bari, Bari, Italy, in 1999. During 1999, she worked with a research contract at the Motorola Florida Research Laboratory, From 2000 to 2004 she worked, with a research contract at University of Ancona, Italy, (now the Universita Politecnica delle Marche), on the development of numerical tools applied to different electromagnetic problems. Since January 2005 she has a tenure position as researcher at Università Politecnica delle Marche. She teaches EMC, antenna design and fundamentals of electromagnetics. Her current research interests include the application of numerical modeling to EMC problem, reverberation chamber, and new antenna design such as plasma antennas. Dr.Russo is a member of IEEE EMC Society and the Italian Electromagnetic Society (SIEm).

Alfredo De Leo was born in Bari, Italy in 1975. He graduated in Electronic Engineering in 1999 from the University of Ancona (actually Università Politecnica delle Marche) and he received the Ph.D. degree in Electromagnetism and Bioengineering in 2014 from the Università Politecnica delle Marche where he is currently responsible of the Antenna and EMC laboratories. His research activities concerns the development of electromagnetic models, laboratory experiments and numerical simulation techniques related to interactions between electromagnetic fields and biological beings, designing of electromagnetic travel aids for visually impaired people, remote sensing of physiological activities and reverberation chambers. Dr. De Leo is a member of IEEE EMC Society and the Italian Electromagnetic Society (SIEm)

Alina Caddemi (M'13) received the degree in Electronic Engineering (honors) and the Ph.D. degree from the University of Palermo, Italy, in 1982 and in 1987, respectively. In 1984, she joined the Electrical Engineering Dept. at the University of Utah, USA, and in 1985 the Electrical and Computer Engineering Dept. at the University of Colorado, Boulder, USA, as a visiting researcher in the field of microwave bioelectromagnetics. From 1990 to 1998, she was with the Department of Electrical Engineering, University of Palermo, as an assistant professor. In 1998 she joined the University of Messina, Italy, where she is currently Full professor of Electronics and the supervisor of the Microwave Electronics (ELEMIC) Lab. Her current research interests are in the field of temperature-dependent linear and noise characterization techniques for solid-state devices, cryogenic measurements and modeling of field-effect transistors, noise modeling of bipolar and field-effect transistors, neural network and genetic algorithm modeling of devices, design and realization of hybrid low-noise components and circuits. She has authored or co-authored more than 250 papers on international scientific journals and conference proceedings. She has been the partner team leader for several national and international projects. She serves as Associate Editor of the International Journal of Numerical Modelling: Electronic Networks, Devices and Fields and in the Editorial Board of Microwave Review, a publication of the national Society for Microwave Technique, Technologies and Systems and Serbia and Montenegro IEEE MTT-S Chapter. She is involved with the Reviewer's Board of national and international projects and serves as a reviewer for many international journals.

Graziano Cerri is currently full professor of electromagnetic fields at the Department of Electromagnetics and Bioengineering at the Università Politecnica delle Marche. His research is mainly devoted to EMC problems, to the analysis of the interaction between e.m. fields and biological bodies and to plasma antennas. Since 2006 to 2014 he was director of the PhD school "Engineering Sciences" of the Engineering Faculty at Università Politecnica delle Marche. Since 2004 he is director of ICEmB (Interuniversity Italian Center for the study of the interactions between Electromagnetic Fields and Biosystems). He is also Member of the Administrative and Scientific Board of CIRCE (Interuniversity Italian Research Centre for Electromagnetic Compatibility), and member of the Scientific Board of SIEm (Italian Association of Electromagnetics). Since 2006 to 2014 he was also member of the steering committee of the EMC-Europe – International Symposium on Electromagnetic Compatibility. Mr. Cerri is also a member of IEEE and of AEI (Italian Electrotechnical and Electronic Association).